Piezo-Semiconductive Quasi-1D Nanodevices with or without Anti-Symmetry

*Rodolfo Araneo, Giampiero Lovat, Paolo Burghignoli, and Christian Falconi**

Stress can modify the charge transport within piezoelectric semiconductors as well as through junctions between piezoelectric semiconductors and other materials. For instance, stress-induced piezopotential can turn an electrically passive nanowire into an electrical energy source[1,2] (e.g., suitable for powering sensors and electronic interfaces)[3]; moreover, in piezotronic and piezophototronic devices stress may change the Schottky barrier heights and the width of depletion/accumulation regions at junctions between the piezo-semiconductor and adjacent materials.[4–10] However, despite significant efforts have already given precious information,[11,12,4] at present, in the absence of sufficiently accurate models, fabricated devices are largely sub-optimal. These remarks apply to even the simplest and most widely used mechanical input for quasi-1D piezo-semiconductive nanostructures, that is axial stress.[4,11] In this paper, we observe that floating electrodes may result in higher piezopotential and conversion efficiency; afterwards, we show that, as an effect of the piezo-semiconductive equations, the piezopotential in homogeneous, floating, quasi-1D piezo-semiconductive nanostructures under axial stress is an anti-symmetric (i.e., odd) function of force. Moreover, adopting typical simplifications (i.e., by assuming ideal ohmic contacts and neglecting both surface states and other anomalies), we explain why this anti-symmetry may be not optimal for designing devices with the highest possible on-off ratios. Finally, we demonstrate that breaking the anti-symmetry can also result in better nanogenerators, piezotronic and piezophototronic devices.

Figure 1a shows our model, consisting of a nanowire surrounded by free space and subject to axial forces. Though some devices rely on different types of mechanical solicitations (e.g., lateral deflection), we deal with nanodevices under purely vertical compression/traction. For instance, one of the most typical arrangements reported for piezotronic devices[4,5] consists in fixing (e.g., with silver-paste) the two ends of a single nanowire on a flexible substrate; when the substrate is bent, assuming that the radius of curvature of the substrate is much larger than the nanowire length (as it is usually the case), an almost purely tensile/compressive strain is generated in the nanowire.[4]

The fully-coupled non-linear partial differential equations to be solved are

$$\begin{aligned} \nabla \cdot \sigma &= 0 \\ \nabla \cdot \mathbf{D} &= q\left(N_{\mathrm{D}}^{+} + p - N_{\mathrm{A}}^{-} - n\right), \end{aligned} \tag{1}$$

where $\mathbf{D} = D_j\,\mathbf{e}_j$ is the electric induction field, $\sigma = \sigma_{ij}\,\mathbf{e}_i \otimes \mathbf{e}_j$ is the stress tensor, q is the magnitude of electron charge, N_{D}^{+}, N_{A}^{+}, n, and p are the ionized donors, ionized acceptors, free electrons, and holes concentrations, respectively. The constitutive equations are

$$\begin{aligned} \sigma_{ij} &= c_{ijkl}^{\mathrm{E}}\varepsilon_{kl} - e_{kij}\,E_k \\ D_j &= c_{jkl}\varepsilon_{kl} + \kappa_0\kappa_{jk}^{\varepsilon}\,E_k \end{aligned} \tag{2}$$

where c_{ijkl}^{E}, e_{jkl}, and $\kappa_{jk}^{\varepsilon}$ are the elastic, piezoelectric, and dielectric tensors, respectively (repeated summation index convention), E_k is the electric field and ε_{kl} is the strain tensor. We fully take into account n and p free charges in the piezo-semiconductor,[12] whose redistribution under thermodynamic equilibrium is given by the Fermi-Dirac statistics (which introduces a non-linearity in the Poisson equation), where the valence and conduction band levels $\varepsilon_{\mathrm{v}}(\mathrm{x})$ and $\varepsilon_{\mathrm{c}}(\mathrm{x})$ are functions of the spatial coordinates x.[12–14] In particular, we assume the band edge shift $\Delta\varepsilon(\mathrm{x})$ as the sum of the electrostatic energy part qV and the deformation potential term, i.e.,

$$\Delta\varepsilon(\mathrm{x}) = \varepsilon_{\mathrm{o}}(\mathrm{x}) - \varepsilon_{\mathrm{o}0} = \varepsilon_{\mathrm{v}}(\mathrm{x}) - \varepsilon_{\mathrm{v}0} = -q\,V + a_{\mathrm{def}}\frac{\Delta\upsilon}{\upsilon_0}, \tag{3}$$

where V is the electrostatic potential and $a_{\mathrm{def}}\frac{\Delta\upsilon}{\upsilon_0}$ is the band-edge shift due to the deformation, proportional to the relative volume change $\frac{\Delta\upsilon}{\upsilon_0}$ through the constant a_{def}.[13] For higher accuracy we consider both anisotropy and the converse piezoelectric effect. The system of nonlinear equations is solved numerically (Supplementary Information). Due to both the very large number of surface states and unpredictable residual stress, metal-piezosemiconductor junctions can behave as Schottky barriers or ohmic contacts; however, since our priority is providing insight for design, we restrict our analysis to static calculations,[11–13] consider an open-circuit (i.e., no load) condition,[11–13,15] ideal ohmic contacts at both terminals,[11–13,15] and zero surface states and intrinsic strain (e.g., due to packaging). Moreover, we neglect thermal effects and all dissipative

Dr. R. Araneo, Dr. G. Lovat
DIAEE–Electrical Engineering Division
"Sapienza" University of Rome
Via Eudossiana 18, 00184, Rome, Italy
Dr. P. Burghignoli
Department of Information Engineering
Electronics and Telecommunications
"Sapienza" University of Rome
Via Eudossiana 18, 00184, Rome, Italy
Dr. C. Falconi
Department of Electronic Engineering
University of Tor Vergata
Via del Politecnico 1, 00133, Rome, Italy
E-mail: falconi@eln.uniroma2.it
Dr. C. Falconi
CNR IDASC
Via Fosso del Cavaliere, 100, 00133 Rome, Italy

DOI: 10.1002/adma.201104588

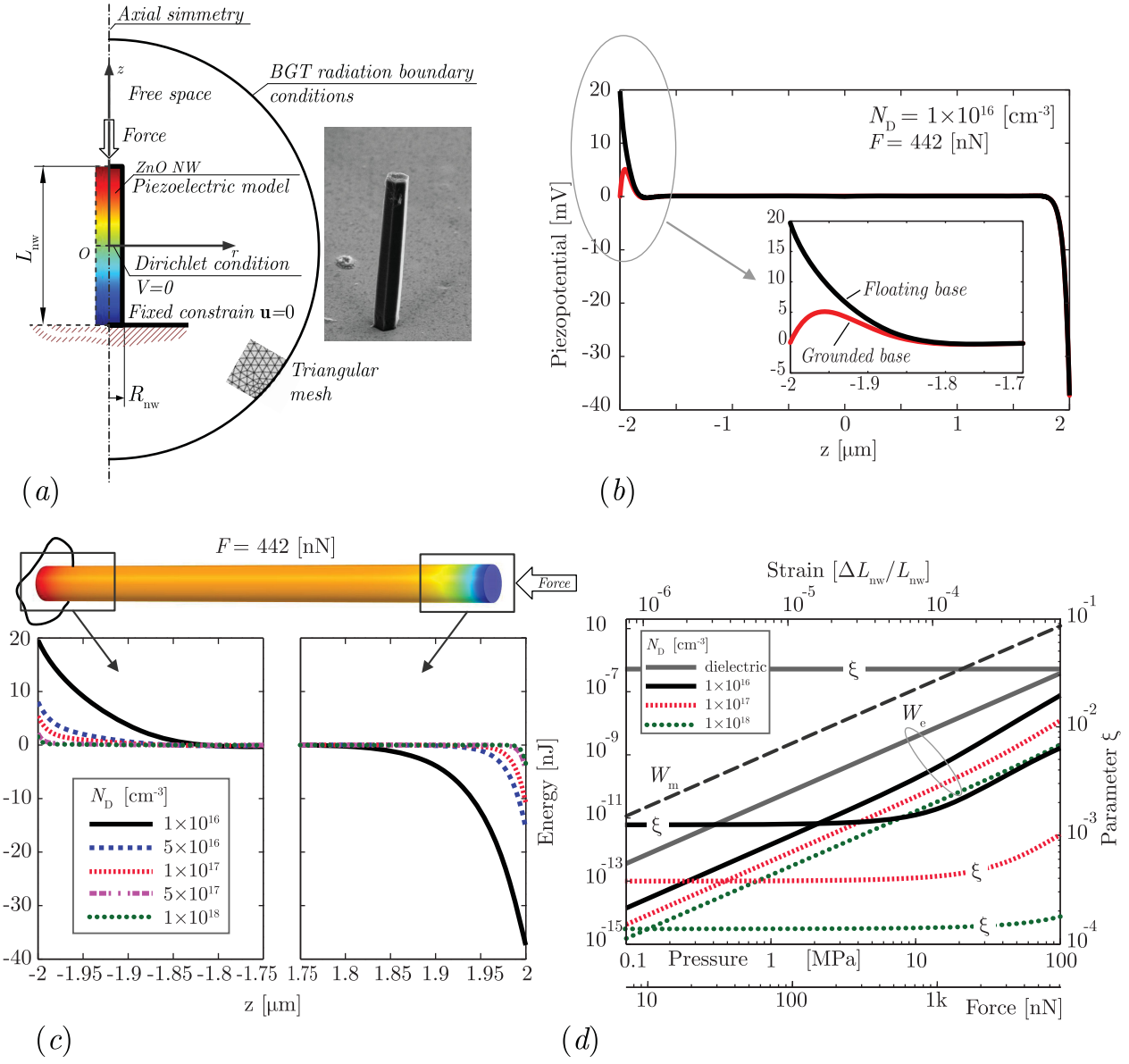

Figure 1. Cylindrical nanowire (radius 150 nm and length 2 μm) surrounded by free space and subject to compressive force. a) View and schematic of the nanowire under analysis. b) Piezopotential along the entire axis of the nanowire with floating and grounded base. c) Piezopotential along the axis of the nanowire in the top and bottom regions for different doping concentrations under a 442 nN[12] compressive force. d) Electrostatic energy W_e, mechanical energy W_m, and ratio ξ between electrostatic and total energies as a function of force/pressure/strain.

mechanisms. We choose ZnO as it has been most widely used for fabricating piezo-semiconductive nanodevices because of its advantages, including its mechanical and optical properties, easy fabrication with low-temperature, low-cost, large-area, and CMOS/MEMS-compatible hydrothermal methods. However, our methodology and conclusions can easily be extended to other materials.

First, we have calculated the piezopotential for a cylindrical *n*-type ZnO nanowire under axial compression (F = –442 nN,[12] $N_D = 10^{16}$ cm^{-3}); the values of all the relevant geometric and physical parameters used in the numerical simulations are given in the Supplementary Information. Figure 1b shows the piezopotential along the axis of the nanowire in both the cases of grounded and floating bottom electrode (the tip is floating in all cases); both the total voltage difference and the stored electrostatic energy are clearly higher for the floating case. Though the bottom electrode potential may be fixed at zero[12] (consistently with experiments where the bottom electrode is connected to ground), here we restrict to floating tip and base electrodes which corresponds to not applying any other boundary condition on the electrical potential except, obviously (general solution for Laplace's equation for charged structures of finite dimensions), the zero value at infinity (enforced by means of open boundary conditions). With floating electrodes, since the typical conductivity of the weakly enhanced base of the nanowire is not so high that there may be no significant voltage

Adv. Mater. **2012**,
DOI: 10.1002/adma.201104588

drop in the enhanced part, two non-negligible voltage drop regions are present; clearly, the higher voltage drop is in the depleted part (Figure 1b). Figure 1c shows the piezopotential for *n*-type doping levels ranging from 10^{16}cm^{-3} to 10^{18}cm^{-3} (for clarity, throughout the paper, we only show the extreme parts of the nanowire where the voltage drops are confined).

Figure 1d shows the stored electrostatic energy W_e and mechanical energy W_m as functions of pressure (or, equivalently, strain or force) for three different doping levels and for an hypothetical nanowire without free charges (as a limiting case, see also Figure S2-S3); W_e, W_m, and the parameter ξ have been computed according to

$$\begin{aligned} W_m &= \int_{V_{nw}} \frac{1}{2} c^E_{ijkl} \varepsilon_{ij} \varepsilon_{kl} d\Omega \\ W_e &= \int_{V_{nw}+V_{fs}} \frac{1}{2} \kappa^{\varepsilon}_{ij} E_i E_j d\Omega \\ \xi &= \frac{W_e}{W_m + W_e}, \end{aligned} \tag{4}$$

where V_{nw} and V_{fs} are the volumes of the nanowire and surrounding free-space, respectively.[16]

Only a fraction of W_e may be transferred to a load and, moreover, dissipative mechanisms may be present; therefore, ξ represents an upper bound to the ability of the piezoelectric nanostructure to convert mechanical energy into electrical energy at low frequencies; ξ is obviously a key parameter for nanogenerators, but may also concisely quantify the electromechanical coupling efficiency in other piezotronic or piezophototronic devices. Remarkably, W_e, W_m, and ξ have been computed for several configurations, but only for purely insulating devices;[11,15] though, clearly, free charges are expected to reduce both the piezopotential and ξ, it was never reported before how large this reduction could be and if there may be methods for increasing ξ in practical devices. As shown in Figure 1d, W_m is proportional to the squared strain and is, obviously, not affected by doping; at all doping levels, ξ is almost constant at low strains and gradually increases with strain (a saturation is reached at very high strain, where linear elastic mechanical models may become questionable). In fact, the total polarization charge Q_{PZ} is proportional to strain; additionally, in each voltage drop region, the voltage drop obviously depends on Q_{PZ}. W_e may be computed as the energy required to move charges from the equilibrium no-stress condition to the final state

$$W_e = \int_0^{Q_{PZ}} V(Q) dQ \tag{5}$$

Since zero polarization charge corresponds to zero voltage drop, for small strains we may use the truncated Taylor expansion

$$V(Q) = \frac{1}{c} Q + O[Q^2], \tag{6}$$

where c has the dimension of a capacitance. Therefore, for small strains

$$W_e \cong \int_0^{Q_{PZ}} \frac{Q}{c} dQ = \frac{Q_{PZ}^2}{2c} \tag{7}$$

Since the magnitude of Q_{PZ} is proportional to the magnitude of strain, similar to W_m, at low strains W_e is also proportional to the squared strain, and therefore, consistently with Figure 1d, ξ is constant at low strains. At very small strains, an increase in the strain results in additional depletion or enhancement charges very close to the junction; at sufficiently higher strains, a further increase in the strain results in additional depletion or enhancement charges located at larger distances from the junction which may be intuitively seen as a reduction of c and, therefore (Q_{PZ} is always proportional to strain), in a relatively larger increase of W_e or, equivalently, in an increase of ξ (though easy to visualize, this is not strictly correct; actually, c is constant, but other terms of the Taylor expansion in Equation (6) will become not negligible and give a similar effect). The proportionality between electrostatic energy and the squared strain at low strains also applies to structures with non-homogeneous sections discussed below.

Figure 1d also reveals that at all strain (or, equivalently, pressure) levels, both W_e and ξ are higher for lower doping levels; in particular, not only the low strain value of ξ is higher for lower doping, but the threshold strain above which ξ increases with strain is also lower for lower doping levels.

In the literature, only *n*-type nanowires under compressive strains and with grounded base have been investigated by FEM calculations when considering free charges.[12] **Figure 2** shows, with floating electrodes, the switch of the two voltage drop regions under change of doping type or of stress sign; for clarity, we have chosen $\Delta\varepsilon_D = \Delta\varepsilon_A = 35$ meV, so that, apart the sign, the only (weak) numerical difference between *n*-type and *p*-type is due to the different effective hole and electron masses, which however is practically negligible. In fact, the inset in Figure 2 shows that, at all pressure (or, equivalently, strain) levels the magnitude of the total voltage difference between the tip and the base is practically equal for *n*- or *p*-type, tensile or compressive strain. Consistently with other studies,[17] from Figure 1b and 2 we conclude that the sign and magnitude of the piezopotential under traction and compression can be related to their doping type and doping levels, respectively.

With floating and cylindrical nanowires under axial stress, qualitatively, the piezo-semiconductor will be depleted at one junction and enhanced at the other junction;[4,5] no axial stress can act on a single junction only; moreover, Figure 1 shows that with typical doping levels, both the voltage drop regions are important. Furthermore, Figure 2 demonstrates that the voltage between the tip and base of the floating nanowire is an odd function of force (or strain), thus revealing anti-symmetry for traction and compression; an applied (axial) stress will unavoidably have effects on both the junctions and reversing the sign of stress will reverse the sign of the voltage between tip and base (this result holds for any strain magnitude). Such anti-symmetry may or may not be desirable and is a direct consequence of the piezo-semiconductive equations in case of two floating, nominally identical junctions under similar stress (enhancement or depletion is dictated by orientation of c-axis).[4,5] However, the two voltage drops add "constructively" to give the open circuit output voltage of the strained nanowire, but add "destructively"

ADVANCED MATERIALS
www.advmat.de

www.MaterialsViews.com

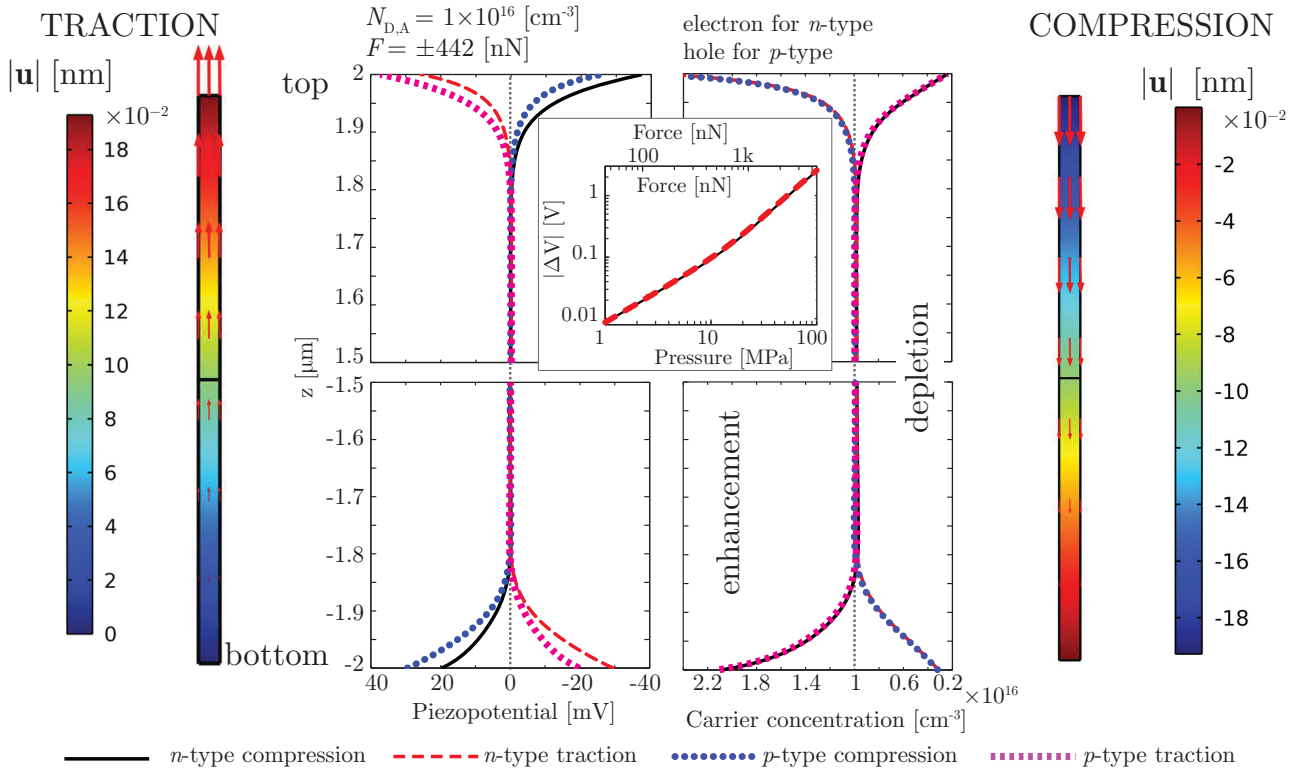

Figure 2. Cylindrical nanowire (radius 150 nm and length 2 μm) surrounded by free space and subject to compressive/tensile force. Displacement, piezopotential, and charge concentrations under traction/compression in n- and p-type cylindrical nanowires. Inset shows the absolute value of the total piezopotential drop between the tip and the base of the wire as a function of force/pressure.

in tuning the conductance of the nanowire, which reduces the on-off ratios. Though in practice other effects (e.g., surface states, residual stress,…) may somehow break the nominal anti-symmetry, it is generally not convenient to rely on spread of parameters for proper operation (e.g., reproducibility would typically be very poor). For instance, a tensile strain would induce depletion at one junction and enhancement at the other one and the two effects would add destructively; moreover, when changing the sign of strain there would still be one junction with depletion and one with enhancement. Therefore, higher on-off ratios can be obtained by piezo-semiconductor devices whose piezopotential-force relationship is not anti-symmetric. Though other strategies may be possible (including the grounded base approach which would, however, reduce both the piezopotential and conversion efficiency), we suggest that non-homogeneous doping and/or sections may effectively break the anti-symmetry; in the following, we focus on quasi-1D piezo-semiconductors with non-homogeneous sections (e.g., truncated conical nanowires, nanotips,…) which may also give substantially higher piezopotential and conversion efficiency for a given applied force as a result of higher strain (when compared with cylindrical nanowires having a cross-section equal to the largest cross-section of the truncated conical nanowire); we do not deal here with fabrication, but only mention that such nanostructures have been extensively reported in the literature. **Figure 3**a shows the *z*-component of the displacement in ZnO nanowires (drawn in different scales because of very different aspect ratios) with $N_D = 10^{16}$ cm^{-3}, compressive 442 nN force (same as for Figure 1b,c,e), circular base with 150 nm radius, and circular tip with radii ranging from 150 nm (i.e., cylindrical nanowire) to 25 nm (much smaller tip radii may result in poor electrical contact). Figure 3b and 3c shows the piezopotential and the charge carrier concentrations at both the tip and base, respectively. As a remarkable difference with respect to cylindrical nanowires, especially for very small radii of the top section, the variations of both piezo-potential and free charge concentrations at the tip are much larger than at the base, as a consequence of the substantially larger pressure (and thus strain) at the narrow tip (in order to maximize the effect, we chose a compressive stress which results in depletion at the narrow tip; effects of traction and compression with both *n*-type and *p*-type doping are not explicitly shown but may qualitatively be deduced from previous discussions). The conical devices exhibit, altogether, a large increase of the piezopotential, an extremely stronger depletion (the charge carrier concentration is reduced by many orders of magnitude, compare Figure 3c and S1), much smaller effects of stress at one junction, and are expected to give higher on-off ratios; additionally, grounding the base of the conical nanowire has almost no effect on the efficiency because the stored energies at the tip largely dominate. In comparison with very thin nanowires, conical nanowires are expected to have significantly better mechanical stability (e.g. buckling).

Figure 3d also shows W_m, W_e, ξ, and the voltage difference between the tip and the base as a function of the applied

Adv. Mater. **2012**,
DOI: 10.1002/adma.201104588

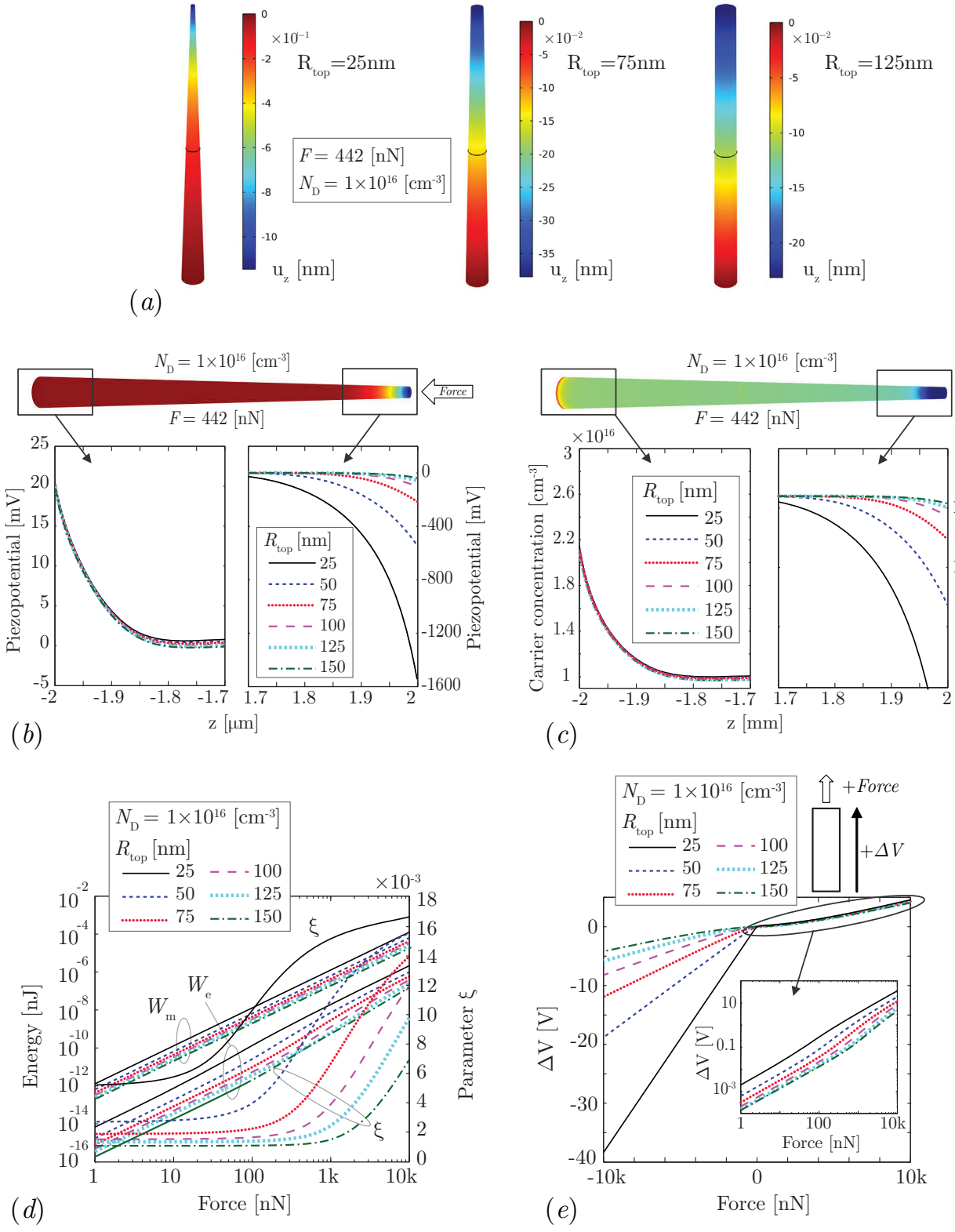

Figure 3. Conical nanowire (bottom radius 150 nm and length 2 μm) surrounded by free space and subject to compressive/tensile force. a) Displacement in truncated conical nanowires with different tip radii. b) Piezopotential at the base (left) and tip (right) of the truncated conical nanowires. c) Carrier concentration at the base (left) and tip (right) of the truncated conical nanowires. d) Electrostatic energy W_e, mechanical energy W_m, and ratio ξ between electrostatic and total energies as a function of force. e) Voltage difference between the tip and base of the nanowire for tensile and compressive forces; as expected, at small tip radii the anti-symmetry is completely lost. Inset shows a zoom of the voltage difference for tensile forces.

compressive force (we use force as the independent variable because pressure is not constant along the devices). As expected from Equation (7), at low force ξ is constant and gradually increases with force. Both ξ and the voltage difference between tip and base significantly increase (for a given force) when compared with the cylindrical nanowire; at 1 μN compressive force, ξ is about 1.6% for the truncated cone with the smallest tip radius and about 0.2% for the cylindrical nanowire. We mention that the pyroelectric coefficient of nanowires for harvesting energy from thermal variations[18] is greatly increased by downscaling; such a strong size effect may affect the pyroelectric parameter for arbitrary shapes when any of its dimensions approaches a critical threshold.[18] Though, similarly, all material properties (e.g., piezoelectric coefficient and Young modulus) may have important size-effects at nanoscale, in absence of sufficiently accurate data, we have used constant coefficients; however we suggest that, in practice, a conical shape may be even more advantageous than predicted by our simulations because of significant size-effects (e.g., piezoelectric coefficients at the narrow tip may be significantly higher).

Figure 3e shows the voltage difference between the tip and base of the nanowire for both compressive and tensile stresses; as expected, in striking contrast with cylindrical nanowires (i.e., tip radius equal to base radius), for nanowires with smaller tip radii the piezopotential-force relation is not anti-symmetric so that, as evident from Figure 3b, the piezopotential is almost exclusively located at the narrow tip and much higher on-off ratios are possible. The breaking-off of the anti-symmetry is due to both the geometry and the coupling of the piezo-semiconductive equations and would not be obtained with insulating piezoelectric conical nanowires (Figure S3d).

In conclusion, we have introduced quasi-1D piezo-semiconductive nanostructures with floating electrodes for maximum piezopotential and efficiency; in these devices we have verified the existence of two voltage-drop regions under axial stress and their switch under change of doping type or of stress sign. We have also given the first (taking into account free charges) estimation for the electrostatic energy stored in axially deformed piezo-semiconductive quasi-1D nanostructures as well as for the ratio between the stored electrostatic and the total (electrostatic plus mechanical) energies, ξ. We have also shown that ξ is almost independent of strain at small strains and increases at higher strains, thus confirming that the ability of nanostructures to withstand extreme deformations without fracture may be very important. Moreover, we have explained why anti-symmetric piezo-semiconductive nanodevices are likely not optimal for maximizing on-off ratios. Finally, we have discussed how non-homogeneous doping and/or sections may break the anti-symmetry and have demonstrated through fully coupled non-linear FEM calculations that piezo-semiconductive nanowires with truncated conical shape and homogeneous doping, upon breaking the anti-symmetry of the piezopotential-force relation, can allow fabricating better nanogenerators, piezotronic, and piezophototronic devices.

Supporting Information

Supporting Information is available from the Wiley Online Library or from the author.

Acknowledgements

This research has been supported by the Italian Institute of Technology (Project Seed - API NANE) and by MIUR (FIRB–Futuro in Ricerca 2010 Project "Nanogeneratori di ossido di zinco ad altissima efficienza per l'alimentazione di microsistemi impiantabili e di reti wireless di sensori"). The authors thank Dr. Giuseppe Romano, Dr. Matthias Auf der Maur, Prof. Aldo Di Carlo, and Prof. Arnaldo D'Amico for their helpful comments.

Received: December 1, 2012
Revised:
Published online:

[1] Z. L. Wang, J. H. Song, *Science* **2006**, *312*, 242.
[2] X. D. Wang, J. H. Song, J. Liu, Z. L. Wang, *Science* **2007**, *316*, 102.
[3] C. Falconi, E. Martinelli, C. Di Natale, A. D'Amico, F. Maloberti, P. Malcovati, A. Baschirotto, V. Stornelli, G. Ferri, *Sens. Actuators B–Chem.* **2007**, *121*, 295.
[4] Y. Zhang, Y. Liu, Z. L. Wang, *Adv. Mater.* **2011**, *23*, 3004.
[5] Z. L. Wang, *Nano Today* **2010**, *5*, 540.
[6] X. D. Wang, J. Zhou, J. H. Song, J. Liu, N. S. Xu, Z. L. Wang, *Nano Lett.* **2006**, *6*, 2768.
[7] J. H. He, C. L. Hsin, J. Liu, L. J. Chen, Z. L. Wang, *Adv. Mater.* **2007**, *19*, 781.
[8] C. S. Lao, Q. Kuang, Z. L. Wang, M. C. Park, Y. L. Deng, *Appl. Phys. Lett.* **2007**, *90*, 262107.
[9] Y. F. Hu, Y. L. Chang, P. Fei, R. L. Snyder, Z. L. Wang, *ACS Nano* **2010**, *4*, 1234.
[10] Y. F. Hu, Y. Zhang, Y. L. Chang, R. L. Snyder, Z. L. Wang, *ACS Nano* **2010**, *4*, 4220.
[11] C. Falconi, G. Mantini, A. D'Amico, Z. L. Wang, *Sens. Actuators B - Chem.* **2009**, *139*, 511.
[12] G. Romano, G. Mantini, A. Di Carlo, A. D'Amico, C. Falconi, Z. L. Wang, *Nanotechnology* **2011**, *22*, 465401.
[13] Y. Gao, Z. L. Wang, *Nano Lett.* **2009**, *9*, 1103.
[14] D. Vasileska, S. M. Goodnick, G. Klimeck, *Computational Electronics*, CRC Press, New York, NY, USA **2010**.
[15] C. Sun, J. Shi, X. Wang, *J. Appl. Phys.* **2010**, *108*, 034309.
[16] B. A. Auld, *Acoustic Fields and Waves in Solids*, Vol. *1*, Wiley, NewYork, NY, USA **1973**.
[17] S. S. Lin, J. H. Song, Y. F. Lu, Z. L. Wang, *Nanotechnology* **2009**, *20*, 365703.
[18] N. Morozovska, E. A. Eliseev, G. S. Svechnikov, S. V. Kalinin, *J. Appl. Phys.* **2010**, *108*, 042009.

DOI: 10.1002/adma.201104588